J Mater Sci: Mater Electron (2015) 26:5243–5253
DOI 10.1007/s10854-015-3059-3

A facile particulate sol–gel route to synthesize nanostructured $CoTiO_3$ thin films and powders and their characteristics

A. Mohammadi[1] · M. Ghorbani[1]

Received: 30 January 2015 / Accepted: 7 April 2015 / Published online: 14 April 2015

Abstract Nanostructured $CoTiO_3$ thin films and powders were prepared by a straightforward aqueous particulate sol–gel route. Titanium(IV) isopropoxide and cobalt chloride were used as titanium and cobalt precursors, respectively. Also, hydroxypropyl cellulose was used as a polymeric fugitive agent in order to increase the specific surface area. The effect of Co:Ti molar ratio and annealing temperature were studied on the crystallization behavior and chemical properties of the products. X-ray diffraction and Fourier transform infrared spectroscopy revealed that the powders crystallized at the low annealing temperature of 300 °C for 1 h, containing anatase-TiO_2, rutile-TiO_2, $CoTiO_3$ and Co_3O_4 phases, depending on annealing temperature and Co:Ti molar ratio. Furthermore, TiO_2 transformation from anatase to rutile phase occurred at 500 °C. The activation energy of crystallite growth was calculated in the range of 3.1–8.5 kJ/mol. Simultaneous differential thermal analysis showed that the final annealing temperature to obtain organic-free cobalt titanate powders could be determined at 560 °C. Field emission scanning electron microscope analysis revealed that the deposited thin films had crystallite and nanostructured morphology with the average grain size in the range 22–32 nm at 500 °C. Atomic force microscopy illustrated 2D and 3D topographies of thin films annealed at 500 °C for 1 h showed that the deposited films had homogeneous, rough structure with nanosized grains.

✉ A. Mohammadi
aida.mohammadi@ut.ac.ir

[1] Department of Materials Science and Engineering, Sharif University of Technology, Azadi Ave., Tehran, Iran

1 Introduction

Metal oxide nanoparticles like titanium dioxide doped with other metallic compounds such as $MTiO_3$ (M:Ni, Fe, Co, Pb and Zn) are generally known as inorganic functional materials due to their multifaceted applications, more particularly in catalysis [1], electronic and photonic materials [2], electrodes of solid oxide fuel cells [3], gas sensors [4], and dynamic random access memories (DRAM) [5]. Particularly, the interest of researchers in $CoTiO_3$ has been increased due to a series of its physiochemical properties, and it is used in a wide variety of applications such as humidity sensors [6], gas sensors, pigment [7], magnetic recording media [8] as well as catalysts. Due to its high dielectric constant, it has also gained attention in the field of semiconductor devices. Conventionally, preparation of $CoTiO_3$ powder involves the solid state reaction between cobalt oxide and titanium oxide at temperature 1100 °C [1]. However, there are many problems associated with this process, such as the high reaction temperature, production of the byproduct titanium oxide, and poor chemical homogeneity of the material obtained. Furthermore, this method is energy-costly, and produces powder particles that are large to process. From various studies, sol–gel is recognized as being the most suitable process over others, because of its lower processing temperature, its low cost, high homogeneity, and purity of resulting materials. Pacheco et al. synthesized a nanocomposite based on the production of nanoparticles of cobalt titanate and titanium oxide by a sol–gel process. XRD analysis demonstrated the stability of cobalt titanate nanocrystals even at temperatures higher than 1000 °C [9]. Cho et al. [10] studied the structural and magnetic properties of $Ti_{1-x}Co_xO_2$ powders by sol–gel process. XRD analysis showed $CoTiO_3$ phase was found above 5 % of Co concentration. He [11]

prepared ultrafine ilmenite $CoTiO_3$ powders using sol–gel method followed by calcining at 700 °C for 3 h. The sol–gel synthesis allowed obtaining cobalt titanate powders as a ceramic pigment in chromaticity. Chaung et al. [12] synthesized $CoTiO_3$ powders by straightforward sol–gel spin-coating method followed by heat treatment at low temperature of 550 °C. The prepared powders were suitable for high-k material application. Enhesarri et al. [13] demonstrated the feasibility of the synthesis of $CoTiO_3$ powders with superparamagnetic behavior at 600 °C for 2 h using sol–gel method containing stearic acid gel. Yang et al. [14] prepared highly crystalline structure $CoTiO_3$ nanofibers which were 200 nm in diameter and several micrometers in length by a sol–gel assisted electrospining method and calcination at 600 °C in air. In all the above mentioned studies polymeric sol–gel process was employed for production of cobalt titanate nanopowders using different Ti and Co precursors, such as tetrabutyl titanate, titanate isopropoxide, cobalt chloride hexahydrate, cobalt acetate, and cobalt nitrate, as well as various solvents such as acetylacetone, ethanol and isopropanol [9–13]. So far no significant work has been reported on application of an aqueous particulate sol–gel route for preparation of $CoTiO_3$ powders and thin films. Furthermore, a strategy for lowering the annealing temperature for crystallization of nanostructured $CoTiO_3$ compound by controlling Co:Ti molar is developed. This process can be defined as an environmentally friendly processing as it uses an aqueous solution. Since the pores in particulate sol–gel processes are much larger than that found in polymeric sol–gel route, the capillary stress and therefore the shrinkage decrease during heat treatment. So, it is possible to produce crack-free thin films with high surface area.

2 Experimental

2.1 Preparation of $CoTiO_3$ sols

Titanium tetraisopropoxide (TTIP) with a normal purity of 97 % (Aldrich, UK), and cobalt(II) chloride Hexahydrate ($CoCl_2{\cdot}6H_2O$) with a normal purity of 99 % (Aldrich, UK) were used as titanium and cobalt precursors, respectively. Analytical grade hydrochloric acid (HCl) 37 % (Fisher, UK) was used as a catalyst for the peptisation and deionised water was used as a dispersing media. Hydroxypropyl cellulose (HPC) (Aldrich, UK) was used as a polymeric fugitive agent (PFA). The $CoTiO_3$ system was prepared by an aqueous particulate sol–gel method. The first step was the preparation of titanium dioxide sol based on our previous study [15]. The water–acid mixture with weight ratio of $HCl:H_2O = 0.04:3.35$ was stabilised at 70 °C, and this temperature was kept constant throughout the experiment, together with continuous stirring. 0.03 mol of TTIP was added, forming a white thick precipitate, which gradually peptised for 2 h to form a clear sol. The clear sol was cooled to room temperature. In separate beakers, predetermined amounts of $CoCl_2{\cdot}6H_2O$ and HPC were dissolved in deionised water at room temperature and stirred for 60 min to obtain the desirable Co:Ti molar ratios, as shown in Table 1.

HPC concentration was defined according to the previous study [16], which induced the highest surface area. This solution was then mixed with TiO_2 sol, stirring for 1 h. All sols were stable and no gelation occurred during preparation. All Sols were characterised in particle size by dynamic light scattering technique (DLS) using a Malvern ZetaSizer 3000 HS at 20 °C using a 10 m WHe–Ne laser, 633 nm wavelength and 90° fixed scattering angle.

2.2 Preparation of $CoTiO_3$ thin films

Films were deposited onto 10 mm × 5 mm × 1 mm quartz substrates for microstructure characterisation. Before deposition, the substrates were cleaned using a high power sonic probe consecutively in water, ethanol and acetone, and dried at 25 °C for 5 min. One layer of film was deposited by dip-coating method. The subsequent heat treatment was optimised as follows. The films were dried at 200 °C for 1 h, annealed at different temperatures (300, 500 and 700 °C) and held at these temperatures for 1 h in air.

2.3 Synthesis of $CoTiO_3$ powders

Powders were prepared by drying each sol at 70 °C temperature for 48 h under a fume cupboard with no special atmosphere. Powders were thermally processed in the same way as the films.

2.4 Structural characterisation

The microstructure of deposited films was characterized using a scanning electron microscope FESEM JEOL 6340 and their topography was investigated by atomic force microscope AFM Nanoscope III, Digital Instrument Inc. The average grain size of the films was determined based on FESEM and AFM micrographs. Powders were characterized in phase composition and crystallite size using an X-ray diffraction diffractometer (XRD) Philips E'pert PW3020, Cu-Kα. The average crystallite sizes of anatase-TiO_2 (matched with database in JCPDS card number of 083-2243), rutile-TiO_2 (matched with database in JCPDS card number of 087-0710), $CoTiO_3$ (matched with database in JCPDS card number of 072-1069) and cubic-CoO

Table 1 Characteristics of prepared sols with various Co:Ti molar ratios

Sample reference	Ti:Co (mol%/mol%)	HCl:Ti (mol%/mol%)	HCl:(Ti + Co) (mol%/mol%)	HPC (g/100 ml)
TiCo31	75:25	0.038:0.351	0.038:(0.351 + 0.004)	0.300
TiCo11	50:50	0.038:0.117	0.038:(0.117 + 0.004)	0.300
TiCo13	25:75	0.351:0.038	0.038:(0.038 + 0.012)	0.300

(matched with database in JCPDS card number of 076-1802) were calculated by the Debye–Scherrer equation [17]:

$$d = K\lambda/\beta\cos\theta \quad (1)$$

where d is the crystallite size, K is a constant of 0.9, λ is the X-ray wavelength of Cu-Kα which is 1.5406 Å, θ is the Bragg angle in degree, and β the full width at half maximum (FWHM) of the peak. The activation energy of crystal growth of $CoTiO_3$ powders can be calculated by Arrhenius equation reported by Bolen and co-worker [18]:

$$\ln(d) = -Q/RT + C \quad (2)$$

where d is the average crystallite size, Q is the activation energy, T is the absolute temperature, R is the ideal gas constant and C is the intercept. Powders were also characterized in thermal behavior using simultaneous differential thermal analysis TA-SDTQ600, with a heating rate of 5 °C/min in air up to 1000 °C and in bond configuration by Fourier transform infrared spectroscopy (FTIR) using a Bruker Optics Tensor 27 analyser in the region 4000–350 cm^{-1}.

3 Results and discussion

3.1 Particle size

Figure 1 shows the mean size of the particles for prepared sols. It can be observed that all sols had a narrow particle size distribution, with particle size of 24, 22 and 26 nm for TiCo31, TiCo11 and TiCo31 sols, respectively. The particle size of the TiO_2 sol reported in our previous study was 18 nm [15]. Therefore, no significant increase in the mean size of the particles was observed for prepared sols, which confirm that stability of sols is maintained when a solution of cobalt chloride is added into TiO_2 sol. To investigate how the hydrodynamic diameter of the particles is affected by ionic strength of the medium various HCl:(Ti + Co) molar ratios, with equal HCl concentrations, were used for different sols. The higher HCl:(Ti + Co) molar ratio, the higher the surface charge around the particles, resulting in the prevention coagulation and flocculation of particles by electrostatic repulsion. However, there is a limit to this behaviour, as an excess of HCl can compress the double layer to such extent that interparticle distance is reduced during collisions, resulting in agglomeration. Therefore, an optimum HCl concentration is required in order to break down the particles into smaller ones during peptisation. Consequently, TiCo11 sol had the smallest particle size amongst all sols.

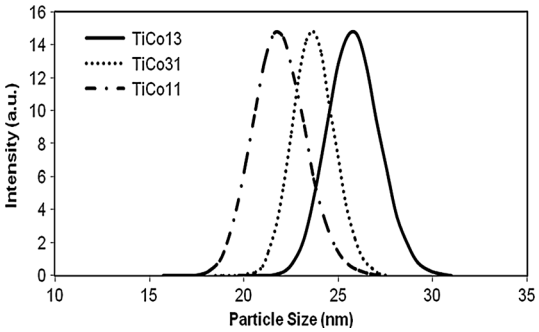

Fig. 1 The mean size of particles in prepared sols

3.2 Thermal analysis

Simultaneous differential thermal analyses (SDT) of cobalt titanate powders are shown in Fig. 2. In addition, the description of peak position and weight loss of all powders determined by this analysis is summarized in Table 2. All powders undergo a dehydration process as located by endothermic peak in the range temperature 56–63 °C, depending upon the Co:Ti molar ratio. Decomposition of the inorganic component such as Cl^- occurs in two steps by endothermic reactions, namely around 113 and 148 °C. The first decomposition step is observed for all powders, whereas the second step is just detected for TiCo13 and TiCo11. The addition of HPC into the sols influences the process of organic decomposition which is shown by a broad exothermic peak at 269, 291 and 294 °C for TiCo13, TiCo11 and TiCo31, respectively. This is consistent with the reported result for the composite TiO_2–HPC powder, being around 300 °C [16]. Further decomposition of organic and inorganic components together with crystallization of cobalt titanate compound is identified by broad exothermic peaks in the range 400–415 °C depending upon the Co:Ti molar ratio. This result is in good agreement with that obtained by XRD analysis regarding crystallization

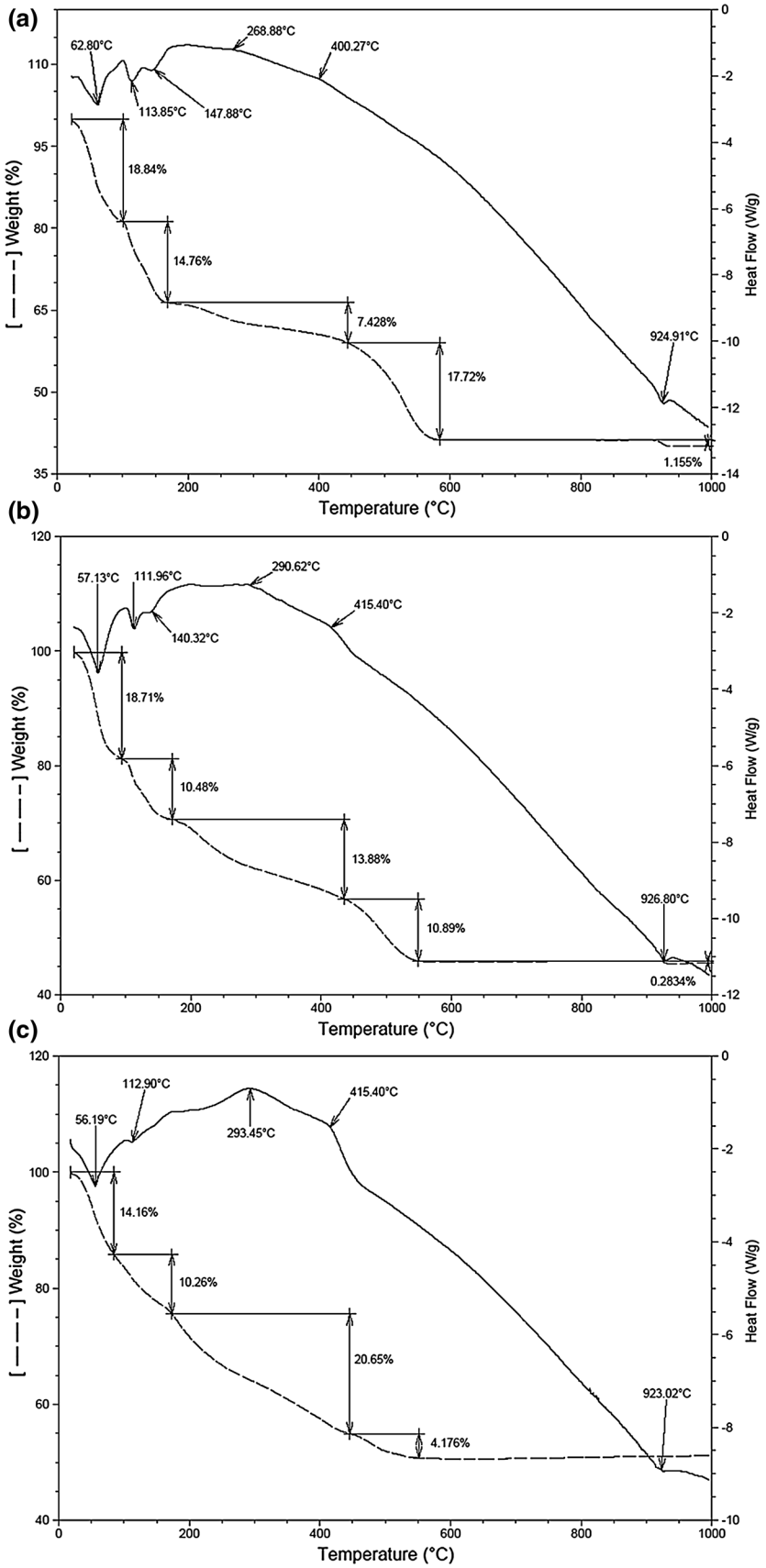

Fig. 2 SDT curves of **a** TiCo13, **b** TiCo11 and **c** TiCo31 powders dried at room temperature for 72 h. The scan rate was 5 °C min^{-1}, performed in air

Table 2 Description of peak position and weight loss for the powders determined by SDT analysis

Stages	TiCo13		TiCo11		TiCo31	
	Peak position (°C)	Weight loss (%)	Peak position (°C)	Weight loss (%)	Peak position (°C)	Weight loss (%)
Water evaporation	62.8	18.8	57.1	18.7	56.2	14.2
First step for decomposition of inorganic compound	113.8	14.8	111.9	10.5	112.9	10.3
Second step for decomposition of inorganic compound	147.9		140.3		–	
Decomposition of HPC and crystallization of cobalt titanate	268.9	7.4	290.6	13.9	293.5	20.7
Further crystallization of cobalt titanate and further decomposition of organic and inorganic compounds	400.3		415.4		415.4	
Decomposition of residual organic compound	–	17.7	–	10.9	–	4.2
Decomposition of cobalt oxide	924.9	1.15	926.8	0.30	923.0	0

temperature of cobalt titanate compound. Finally, decomposition of cobalt oxide can be identified by an endothermic peak around 925 °C, which is consistent with decomposition temperature of cobalt oxide compounds (i.e., CoO, Co_2O_3 and Co_3O_4) reported in the literature [19].

The weight loss of the powders occurs at five stages. In the first stage (below 63 °C), the weight loss is a result of the evaporation of water. In the second stage, from 100 to 180 °C, the weight loss is ascribed to the decomposition of the inorganic component. Decomposition of HPC accompanied with further decomposition of inorganic component occurs in the third stage in the range 180–440 °C. In the fourth stage between 440 and 560 °C, the weight loss is attributed to decomposition of residual organic compounds, arising from HPC. In the last stage above 900 °C, the low weight loss can be related to the decomposition of cobalt oxide. Since the prepared cobalt titanate powders showed good crystalline structure at 300 °C and the decomposition of residual organic and inorganic components occurred in the fourth stage, it can be concluded that the ultimate annealing temperature to obtain organic and inorganic free cobalt titanate powders can be determined at 560 °C.

3.3 Infrared characteristics

The bond configuration of $CoTiO_3$ powders sintered at 300 °C for 1 h is shown in Fig. 3. It is known that the absorption bands in the range 1100–1000 cm^{-1} are attributed to the OR groups linked to Ti such as OC_3H_7, OC_4H_7 and OC_2H_5 [20]. The characteristic absorption peak of (OR) group of titanium isopropoxide, which was the precursor of the sols, is in range 1080–1050 cm^{-1} [21]. Owing to the fact that no absorption peak was detected in this range for both annealing temperature, it is concluded that all four (OR) groups of titanium isopropoxide were substituted with (OH) groups of water. Thus, a full conversion of TTIP is obtained by the hydrolysis reaction, resulting in formation of TiO_2 particles. The band due to the Ti–O stretching vibration is found in the range 600–400 cm^{-1} [21]. Therefore, the absorption band at 567 cm^{-1} for TiCo31, 597 cm^{-1} for TiCo11 and 555 cm^{-1} for TiCo13 powders are considered to be the above stretching vibrations, corresponding to the presence of TiO_6 group. The band at 1458 cm^{-1} is due to the stretching vibration of the C–H bond of organic compounds (i.e., HPC) [21]. Moreover, the absorption peak at 2025 cm^{-1} is due to the vibration of C=C=O [21]. Water incorporation is found with the peak in the range 1643–1604 cm^{-1} for all powders [20]. It is known that the broad band in the range 3520–3097 cm^{-1} is due to the stretching vibration of the hydroxyl (O–H) bond. The absorption band at 2372 cm^{-1} is attributed to CO_2 gas from atmosphere.

3.4 Crystal characterization

Figure 4 shows the X-ray diffraction patterns of the powders annealed in the range 300–700 °C for 1 h. In addition, the distribution of phases determined by XRD is summarised in Table 3. The anatase-TiO_2 and the rutile-TiO_2 have tetragonal structure, whereas cobalt oxide (Co_3O_4) and cobalt titanate ($CoTiO_3$) have cubic and rhombohedral structures, respectively. It is evident that phase composition of the powders depends on Co:Ti molar ratio and annealing temperatures. TiCo13 and TiCo31 powders annealed at 300 °C showed a crystalline structure containing mixtures of $CoTiO_3$, anatase-TiO_2, and Co_3O_4 phases, while TiCo11 powder annealed at the same temperature showed a crystalline structure with TiO_2-anatse and $CoTiO_3$ phases. At 500 °C, $CoTiO_3$ phase with a mixture of anatase-TiO_2 and rutile-TiO_2, $CoTiO_3$ and Co_3O_4, and $CoTiO_3$ phase were formed for TiCo31, TiCo13, and

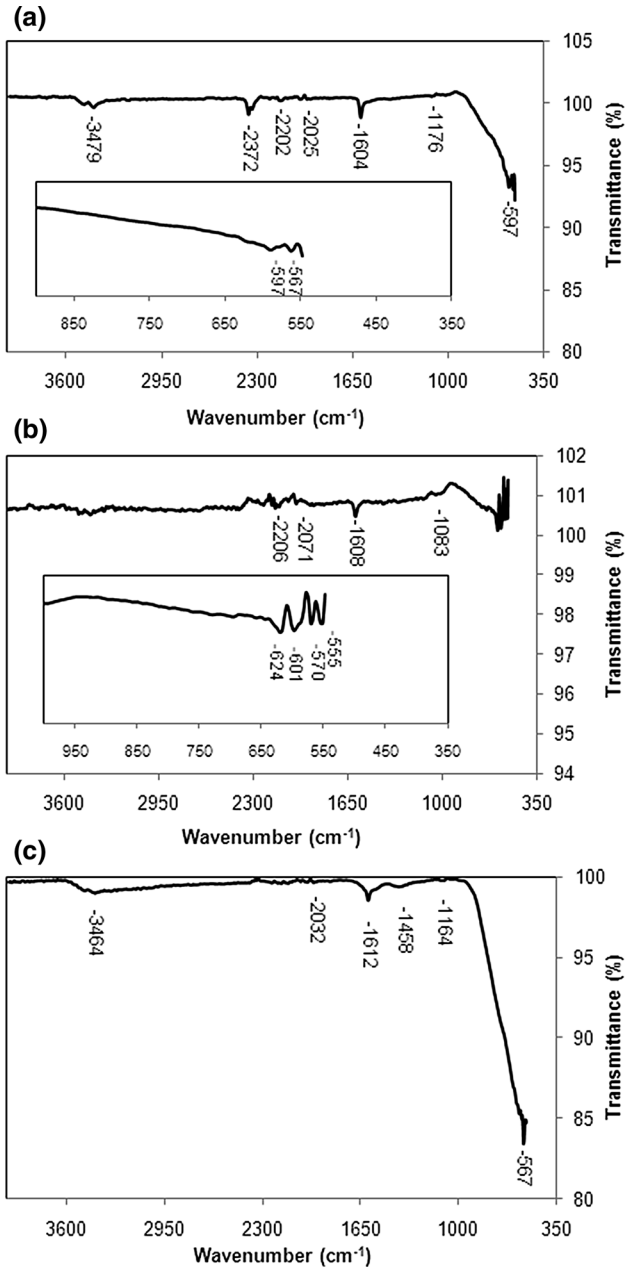

Fig. 3 FTIR spectra of $CoTiO_3$ powders annealed at 300 °C: **a** TiCo13, **b** TiCo11 and **c** TiCo31

TiCo11 powders, respectively. Anatase to rutile phase transformation is negligible at temperatures higher than 500 °C [15]. Furthermore, at T ≥ 500 °C, TiCo11 powder had crystallite and pure phase of $CoTiO_3$, which indicated that crystalline $CoTiO_3$ powders were produced at the low temperature of 500 °C. Figure 5 illustrates the effect of Co:Ti molar ratio and annealing temperatures on the crystallite size of the prepared powders. As can be seen, the crystallite size of all powders was increased by increasing the annealing temperature as a result of the sintering of particles. Furthermore, $CoTiO_3$ phase had the smallest crystallite size for the powder containing equal molar ratio of Co:Ti (i.e., 50:50) at 300 °C, while it had the smallest crystallite size for the powder containing Co:Ti molar ratio (i.e., 25:75) at 500 and 700 °C. The effect of Co:Ti molar ratio and annealing temperatures on the phase percentage of the powders sintered in the range 300–700 °C for 1 h is shown in Fig. 6. As can be seen, TiCo31 powder annealed at 300 °C had TiO_2-anatase dominant phase with the percent of 73 %, 27 % of $CoTiO_3$, and 8 % of Co_3O_4. By increasing the annealing temperature to 700 °C, phase percentage of $CoTiO_3$ was increased to 56 %. In addition, TiCo11 powder annealed at 300 °C showed a mixture of $CoTiO_3$ (96 %) and TiO_2-anatase (4 %) phases. At T ≥ 500 °C, the pure phase of $CoTiO_3$ was formed and the phase percentage of TiO_2-anatase was decreased. TiCo13 powder annealed at 300 °C had Co_3O_4 dominant phase with the percent of 76 %, 15 % of $CoTiO_3$, and 9 % of TiO_2. By increasing the annealing temperature up to 700 °C, the phase percentage of $CoTiO_3$ was increased to 40 %. Figure 7 shows a plot of logarithm of average crystallite size versus the reciprocal of absolute temperature. Based on the slope of the lines, the activation energy of crystallite growth for $CoTiO_3$, Co_3O_4 and TiO_2 phases were calculated as 4.2, 3.1, and 8.5 kJ/mol, respectively. Therefore, the small calculated activation energies of the powders denotes on the fact that nano-sized grains have higher surface area to volume ratios compared to bulk materials, which increases the total surface energy. Thus, less energy is required to induce the crystal growth.

3.5 Microstructure

3.5.1 FE-SEM analysis

Figure 8 shows surface micrographs of sol–gel prepared thin films annealed at 500 °C for 1 h. It can be observed that all deposited films had crystalline structure, which is in good agreement with the XRD results. In all cases, relatively dense, homogeneous, nanograins and crack-free films were obtained. This could be supported by the fact that employment of water with low evaporation rate, as dispersant media, has kept films crack free. In addition, the interstices between the particles caused by HPC are noticeable resulting in a porous structure with irregular pore shape. It is evident that, the porosity percentage of the films increased with an increase of Co:Ti molar ratio. This can be explained by the fact that the decomposition of cobalt chloride is an endothermic reaction (as confirmed by SDT analysis in Sect. 3.2) and, therefore, the heat is consumed for decomposition of the inorganic compound rather than sintering the particles and reducing the porosity. Therefore, it is possible to control the densification process (i.e., porosity reduction) of $CoTiO_3$ films by Co:Ti molar ratio.

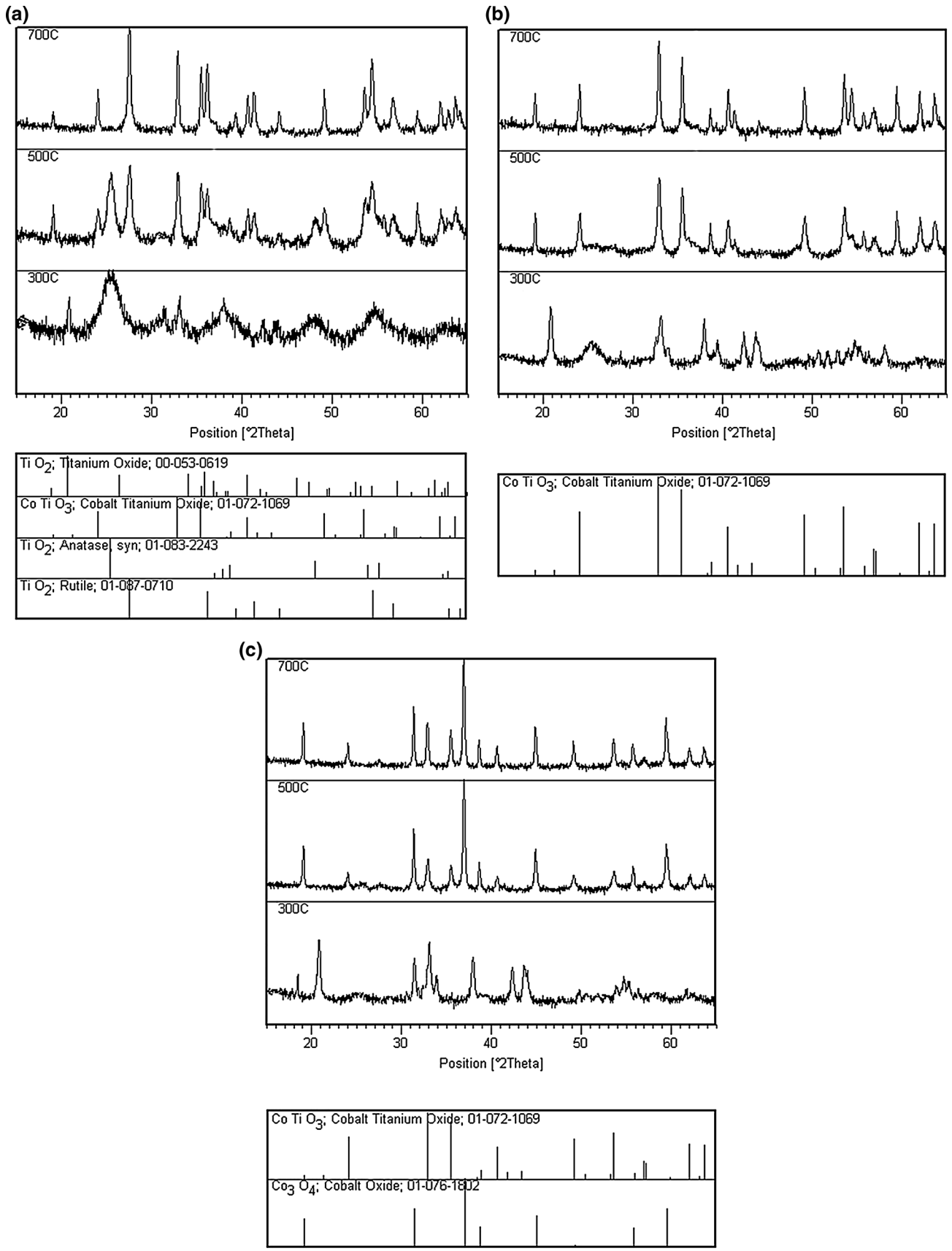
(a)
700C
500C
300C
20
30
40
50
60
Position [°2Theta]
Ti O2; Titanium Oxide; 00-053-0619
Co Ti O3; Cobalt Titanium Oxide; 01-072-1069
Ti O2; Anatase, syn; 01-083-2243
Ti O2; Rutile; 01-087-0710
(b)
700C
500C
300C
20
30
40
50
60
Position [°2Theta]
Co Ti O3; Cobalt Titanium Oxide; 01-072-1069
(c)
700C
500C
300C
20
30
40
50
60
Position [°2Theta]
Co Ti O3; Cobalt Titanium Oxide; 01-072-1069
Co3 O4; Cobalt Oxide; 01-076-1802

◄**Fig. 4** XRD patterns of $CoTiO_3$ powders annealed in the range 300–700 °C: **a** TiCo31, **b** TiCo11 and **c** TiCo13

size amongst all films. These results are consistent with those obtained by XRD analysis, given that TiCo11 powder possessed the smallest crystallite size.

Table 3 Distribution of phases for prepared powders determined by X-ray diffraction

Powder	300 °C	500 °C	700 °C
TiCo31	$CoTiO_3 + Co_3O_4 + TiO_2$(A)	$CoTiO_3 + TiO_2$(A,R)	$CoTiO_3 + TiO_2$(R)
TiCo11	$CoTiO_3 + TiO_2$(A)	$CoTiO_3$	$CoTiO_3$
TiCo13	$CoTiO_3 + Co_3O_4 + TiO_2$(A)	$CoTiO_3 + Co_3O_4$	$CoTiO_3 + Co_3O_4$

A, anatase-TiO_2; R, rutile-TiO_2

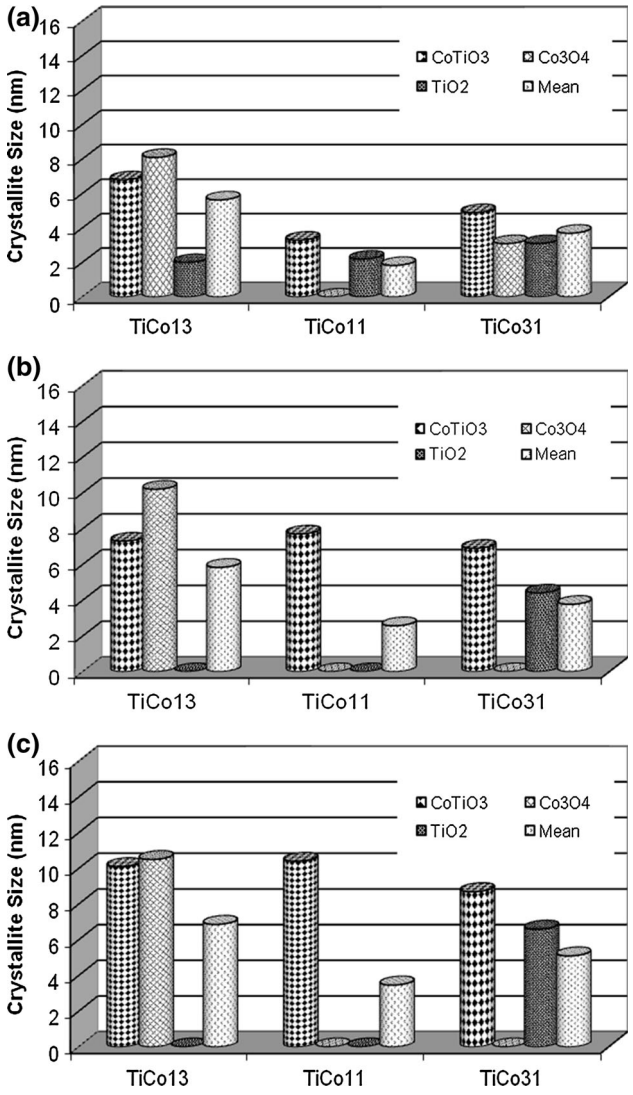

Fig. 5 The effect of Co:Ti molar ratio on crystallite size of the powders sintered in the range 300–700 °C for 1 h

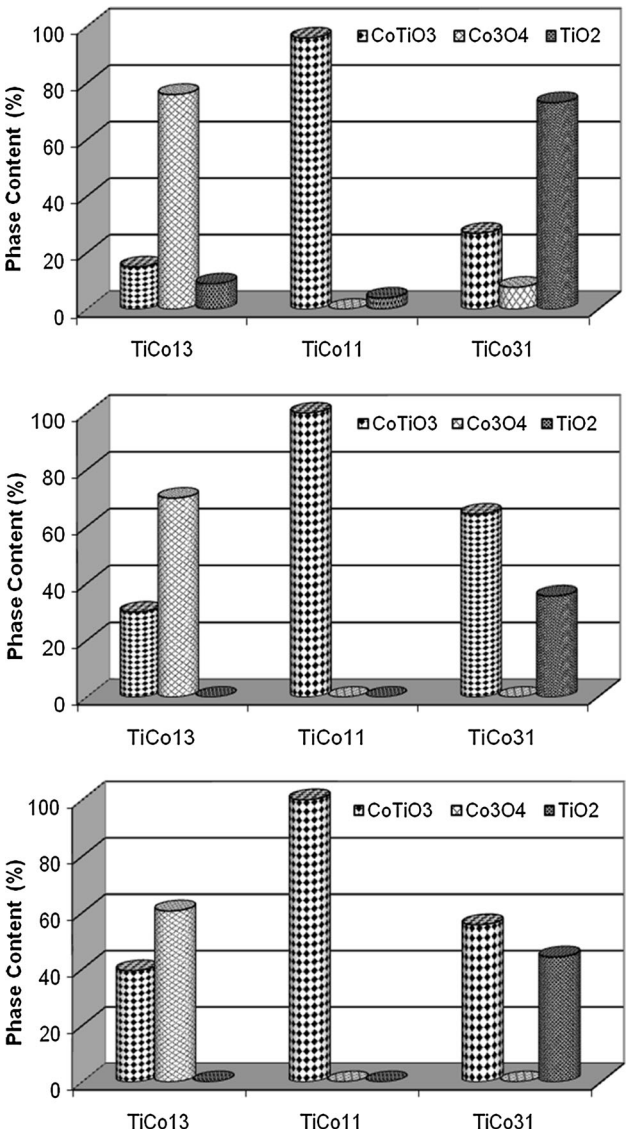

Fig. 6 The effect of Co:Ti molar ratio on phase compounds of the powders sintered in the range 300–700 °C for 1 h

The average grain size of the films annealed at 500 °C is around 30 nm for TiCo31, 22 nm for TiCo11 and 32 nm for TiCo13. Thus, TiCo11 film had the smallest grain

3.5.2 AFM analysis

Figure 9 illustrates 2D and 3D topographies of TiCo11 thin film annealed at 500 °C for 1 h. As can be observed

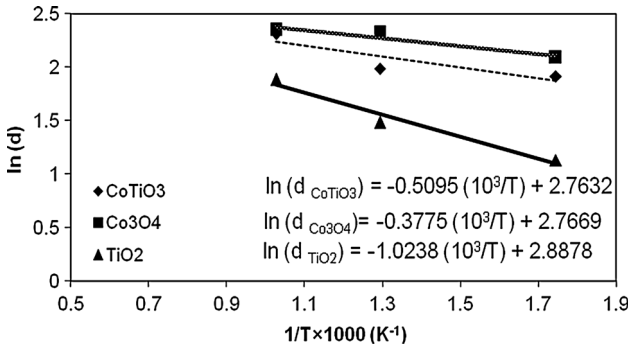

Fig. 7 A plot of ln(d) versus the reciprocal of absolute temperature (1/T) × 1000 to determine the activation energy of crystallite growth of phases annealed for 1 h

in 2D image, the deposited film shows that it is homogeneous, rough and uniform with nanosized grains. Based on 3D image, it can be concluded that the film has a hill-valley like morphology made up of small grains. Moreover, the deposited $CoTiO_3$ compound by a particulate sol–gel process is a nanostructured and porous thin film. The average crystallite size of this thin film is around 20 nm, which is consistent with that obtained by FE-SEM analysis. The roughness mean square (rms) of TiCo11 thin film obtained from 5 μm × 5 μm area was 47 nm. Therefore, the prepared thin film had a high surface area.

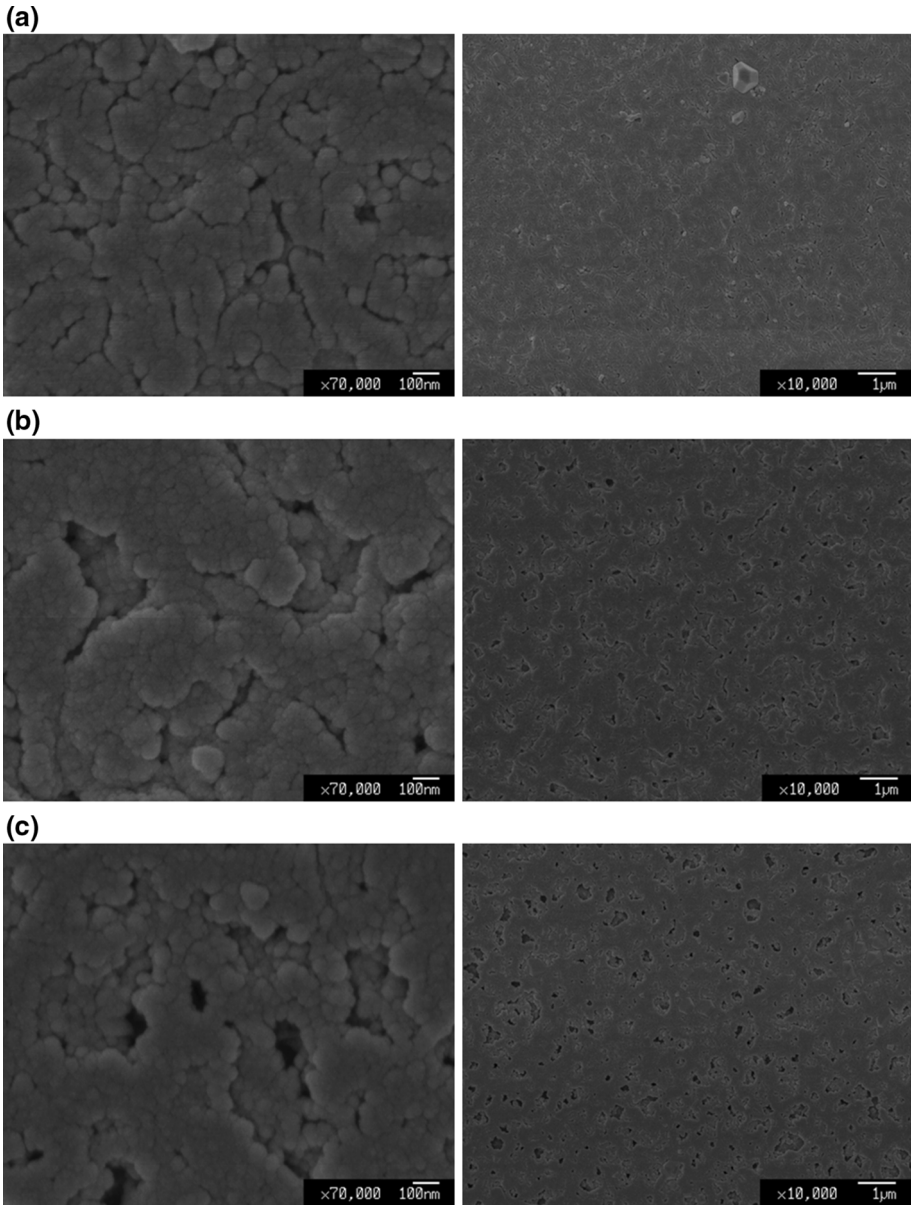

Fig. 8 Surface morphology of deposited films annealed at 500 °C: **a** TiCo13, **b** TiCo11 and **c** TiCo31

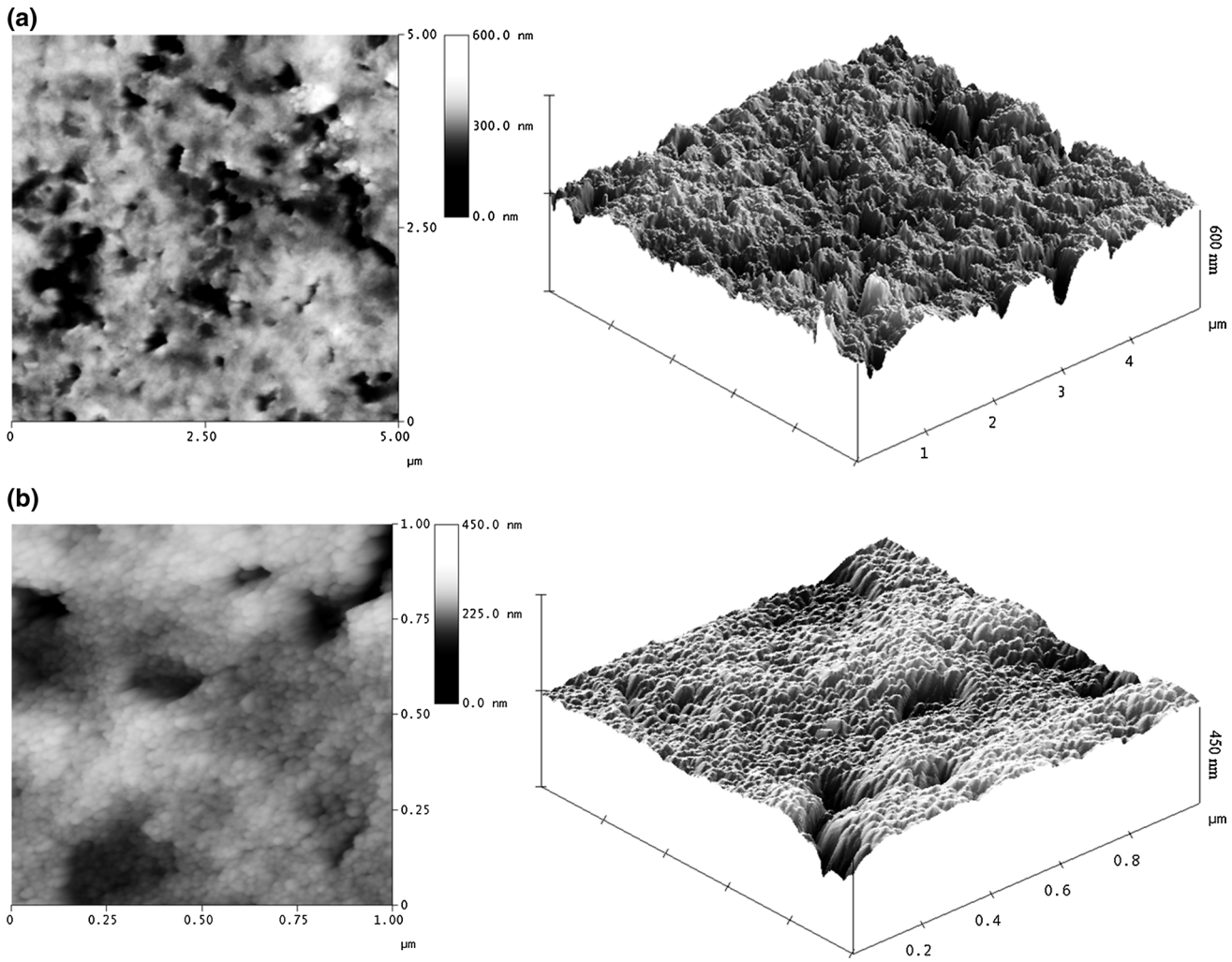

Fig. 9 Atomic force micrographs of TiCo11 film annealed at 500 °C for 1 h: **a** 5 μm × 5 μm and **b** 1 μm × 1 μm

4 Conclusions

$CoTiO_3$ thin films and powders with nanocrystalline structure were prepared by a low temperature and a new water-based sol–gel route. The prepared sols showed a narrow particle size distribution with particle size in the range 22–26 nm. Moreover, the sols were stable over 3 months, since the constant zeta potential was measured during this period. It was found that the phase composition and crystallite size of the samples depends on Co:Ti molar ratio and annealing temperature. X-ray diffraction analysis revealed that cobalt titanate phase was crystallized at the low annealing temperature of 300 °C for 1 h. The average crystallite size of synthesized powders was 3.7 nm at 300 °C and cobalt titanate nanoparticles with 5.1 nm crystallite size were achieved by increasing the process temperature to 700 °C. SDT analysis showed that the final annealing temperature to obtain organic–inorganic free cobalt titanate powders can be determined at 560 °C. FE-SEM and AFM images showed that relatively dense, homogeneous, nanograins and crack-free film was obtained. The present study succeeded in producing $CoTiO_3$ thin films and powders by a simple and low cost aqueous sol–gel route in comparison to the previous studies used by polymer sol–gel process.

Acknowledgments The authors would like to thank Iran Nanotechnology Initiative Council for the financial support.

References

1. T. Kazuyuki, U. Yasuo, T. Shuji, I. Takashi, U. Akifumi, J. Am. Chem. Soc. **106**, 5172 (1984)
2. H.S. Nalwa, *Advanced Electronic and Photonic Materials and Devices* (Academic Press, San Diego, 2001)
3. O. Yamamoto, Y. Takeda, R. Kanno, M. Noda, Solid State Ion. **22**, 241 (1987)
4. M. Siemons, U. Simon, Sens. Actuators B **120**, 110 (2006)

5. T.S. Chao, W.M. Ku, H.C. Lin, D. Landheer, Y.Y. Wang, Y. Mori, IEEE Trans. Electron Devices **51**, 2200 (2004)
6. X. Chu, X. Liu, G. Wang, G. Meng, Mater. Res. Bull. **34**, 1789 (1999)
7. W. Büchner, R. Schliebs, G. Winter, K.H. Büchel, *Industrial Inorganic Chemistry* (VCH, Weinheim, 1989)
8. G. Radnoczi, P.B. Barna, M. Adamik, Z.S. Czigany, J. Ariake, N. Honda, K. Ouchi, Cryst. Res. Technol. **35**, 707 (2000)
9. F. Pacheco, M. Gonzalez, A. Medina, S. Velumani, J.A. Ascencio, J. Appl. Phys. A **78**, 531 (2004)
10. J.H. Cho, B.Y. Kim, H.D. Kim, S.I. Woo, S.H. Moon, J.P. Kim, Y. Chae Ryong Cho, G. John, C. Kim, D.H. Kim, Phys. Stat. Sol (b) **241**, 1537 (2004)
11. H.Y. He, Powder Metall. **51**, 224 (2008)
12. S.H. Chuang, R.H. Gao, D.H. Wang, H.P. Liu, L.M. Chen, M.Y. Chiang, J. Chin, Chem. Soc. **57**, 932 (2010)
13. M. Enhessari, A. Parviz, K. Ozaee, E. Karamali, J. Exp. Nanosci. **5**, 61 (2010)
14. G. Yang, W. Yan, J. Wang, H. Yang, Mater. Lett. **122**, 117 (2014)
15. M.R. Mohammadi, M.C. Cordero-Cabrera, M. Ghorbani, D.J. Fray, J. Sol-Gel Sci. Technol. **40**, 15 (2006)
16. M.R. Mohammadi, M.C. Cordero-Cabrera, D.J. Fray, M. Ghorbani, Sens. Actuators B **120**, 86 (2006)
17. B.D. Cullity, *Introduction to Magnetic Materials* (Addison-Wesley Publishing Company, London, 1972)
18. M. Jarcho, C.H. Bolen, M.B. Thomas, J. Bobick, J.F. Kay, R.H. Doremus, J. Mater. Sci. **11**, 2027 (1976)
19. Z.P. Xu, H.C. Zeng, J. Mater. Chem. **8**, 2499 (1998)
20. T. Ivanova, A. Harizanova, M. Surtchev, Mater. Lett. **55**, 327 (2002)
21. G. Socrates, *Infrared Characteristic Group Frequencies: Tables and Charts* (Wiley, London, 2004)